Heliyon

ELSEVIER

Received:
31 August 2018
Revised:
8 December 2018
Accepted:
6 March 2019

Cite as: Trilok K. Pathak, R. E. Kroon, Valentin Craciun, Marcela Popa, M. C. Chifiriuc, H. C. Swart. Influence of Ag, Au and Pd noble metals doping on structural, optical and antimicrobial properties of zinc oxide and titanium dioxide nanomaterials. Heliyon 5 (2019) e01333. doi: 10.1016/j.heliyon.2019.e01333

Influence of Ag, Au and Pd noble metals doping on structural, optical and antimicrobial properties of zinc oxide and titanium dioxide nanomaterials

Trilok K. Pathak [a,b,**], **R. E. Kroon** [b,***], **Valentin Craciun** [c,e], **Marcela Popa** [d], **M. C. Chifiriuc** [d], **H. C. Swart** [b,*]

[a] *Department of Physics, Teerthanker Mahaveer University, Moradabad, India*

[b] *Department of Physics, University of the Free State, Bloemfontein, South Africa*

[c] *National Institute for Laser, Bucharest, Magurele, Romania*

[d] *Microbiology Immunology Department, Faculty of Biology, The Research Institute of the University of Bucharest (ICUB), University of Bucharest, 77206, Bucharest, Romania*

[e] *Dentix MileniumSRL, Sabareni, Ilfov, Romania*

[*] Corresponding author.

[**] Corresponding author.

[***] Corresponding author.

E-mail addresses: tpathak01@gmail.com (T.K. Pathak), kroonre@ufs.ac.za (R.E. Kroon), SwartHC@ufs.ac.za (H.C. Swart).

Abstract

Oxide materials (ZnO, TiO_2) doped with noble metals were synthesized using the combustion technique. The results of the addition of Ag, Au, and Pd up to a concentration of 2 mol% on the structural, optical, morphological and antimicrobial properties was considered. X-ray diffraction experiments revealed that the crystal structure of the host materials remained unaltered despite doping with noble metals. From the scanning electron microscopy results, it was evident that the doped nanoparticles aggregated in clusters of different sizes in the host

https://doi.org/10.1016/j.heliyon.2019.e01333

matrix. The plasmonic effect was also observed in the absorbance spectra of the different doped materials. The obtained materials have shown promising antimicrobial features. All ZnO materials exhibited a high antimicrobial activity, with very low minimum inhibitory concentration values, against the planktonic growth of all tested Gram-positive and Gram-negative bacterial strains. All doped materials exhibited very good anti-biofilm activity, the lowest minimal biofilm eradication concentration values being registered for ZnO doped with Au and Pd toward *Escherichia coli* and for ZnO doped with Ag against *Candida albicans*. These results indicate the potential that these materials have for antimicrobial applications in the fields of biomedicine and environmental protection.

Keywords: Materials science, Nanotechnology, Materials chemistry, Pharmaceutical science

1. Introduction

The past decades have seen a strong research interest in nanomaterials due to their potential for a wide range of applications, such as for industrial, optoelectronic and biomedical applications, etc. [1, 2, 3]. The ZnO and TiO_2 nanomaterials are among the most studied for antimicrobial applications, due to their large spectrum of anti-infectious activities, including viral, bacterial, fungal and protozoal infections. Direct comparisons of these two materials have been presented by various researchers [4, 5, 6, 7, 8, 9, 10, 11, 12, 13, 14, 15, 16]. One of the mechanisms of their antimicrobial activity is the production of reactive oxygen species (ROS) (i.e., hydroxyl radicals $OH^{\bullet}$, superoxide ions $O_2^{-\bullet}$, and singlet oxygen) particularly under ultraviolet (UV) illumination, causing deleterious effects on microorganisms through peroxidation of cellular constituents like proteins and lipids as well as the loss of membrane integrity [4, 17, 18, 19]. However, the cellular membrane damage could also be due to the direct interaction between the nanoparticles (NPs) and the cell membrane lipids and/or proteins, even in the absence of ROS release [20, 21]. While TiO_2 exhibits excellent chemical stability, ZnO is stable only in a very narrow pH range and it typically releases Zn^{2+} in aqueous solutions [9]. Noble metals such as Ag, Au, Pd are frequently used to modify oxide based semiconductors in order to improve their properties, including the antimicrobial activity. Noble metal doping or incorporation in ZnO has drawn particular attention, due to the specific advantages of this material, although TiO_2 could represent a suitable alternative for ZnO since both materials exhibit similar band-gap energies [22, 23, 24]. Ashkarran [25] synthesized Ag-doped TiO_2 NPs by a two-stage process which proved to be active against *Escherichia coli* under UV and visible light irradiation. Other studies have shown that Ag/TiO_2 NPs proved to exhibit a wide spectrum of antimicrobial activity against several Gram-negative and Gram-positive bacteria, including

https://doi.org/10.1016/j.heliyon.2019.e01333

enteropathogenic *Escherichia coli* and highly resistant strains, such as methicillin-resistant *Staphylococcus aureus* strains [4]. The significant enhancement in the antibacterial properties of Ag/TiO_2 NPs under visible light irradiation has been proved to be directly related to the effect of Ag, which acts as electron traps in the TiO_2 band gap [4]. The antimicrobial activity of Ag/TiO_2 NPs proved to be enhanced in comparison with bare TiO_2 and Ag NPs after incubation in the dark, suggesting that the synergistic effect of the hybrid materials could also occur by a photoactivity−independent mechanism [4].

Previously we have reported on the antibacterial properties of pure (undoped) ZnO synthesized by the combustion method, which was noted to be an effective process to obtain nanocrystalline large surface area material directly without need of further processing or thermal treatment [26]. We have also previously reported the structure and Plasmon absorption properties of ZnO nanocrystalline material with noble metal dopant created by combustion synthesis [27]. Photocatalytic properties of Ag and Au doped ZnO were reported together with limited biological testing [28], while in the present work we consider in detail the antimicrobial properties of Ag, Au and Pd (2 mol%) doped ZnO as well as reporting on the structural, optical and antimicrobial properties of undoped and Au doped (0.5 mol%) TiO_2.

2. Experimental

2.1. Synthesis

Zinc nitrate [$Zn(NO_3)_2.6H_2O$], titanyl nitrate [$TiO(NO_3)_2$], silver nitrate [$AgNO_3$], tetrachloroauric-III-acid hydrate ($HAuCl_4.xH_2O$) and potassium tetrachloropalladate (K_2PdCl_4) were taken as starting chemicals. Dopant and host precursors, with urea ($CO(NH_2)_2$) as fuel, were used to create an aqueous solution with 5 mL of water. While stirring, a gel was formed by heating at 80 °C for 30 min. When this was put in a muffle furnace set to 500 °C, a combustion process occurred shortly thereafter. The product was ground to obtain the oxide nanomaterials.

2.2. Structural and optical characterization

The prepared nanomaterials were characterized in terms of crystal structure using Cu Kα radiation to perform X-ray diffraction (XRD) experiments with a Bruker D8 Advance machine. Morphology of the synthesized NPs was examined by scanning electron microscopy (SEM). An integrating sphere made of spectralon was used with a PerkinElemer Lambda 950 UV−vis spectrophotometer to collect diffuse reflectance (DR) spectra. Photoluminescence (PL) measurements were made at room temperature using a 325 nm emitting He-Cd laser for excitation of the samples.

https://doi.org/10.1016/j.heliyon.2019.e01333

2.3. Antimicrobial activity assay

The tested hybrid nanomaterials, i.e., Ag/ZnO, Pd/ZnO, Au/ZnO, TiO_2, Au/TiO_2 were solubilized in dimethyl sulfoxide (DMSO) for obtaining a stock concentration of 10 mg/mL. The following reference strains were used: Gram-positive bacterial strains (*Staphylococcus aureus* ATCC 25923, *Enterococcus faecalis* ATCC 29212), Gram-negative bacterial strains (*Escherichia coli* ATCC 25922, *Pseudomonas aeruginosa* ATCC 27857) and the yeast strain *Candida albicans* ATCC 10231. The microbial strains were streaked on plate count agar medium incubated at 37 °C for 24 h in order to obtain fresh cultures, from which standardized microbial inocula of 0.5 McFarland density (1-3x10^8 CFU-colony forming units/mL) were prepared in sterile saline.

2.3.1. Qualitative screening of the antimicrobial activity

This was done by an adapted diffusion method consisting of spotting a volume 10 μL of the stock solutions on Muller-Hinton agar medium previously seeded with the microbial suspension. The plates were allowed to incubate at room temperature for 15−20 min for the adsorption of the solution drop into the medium, and then incubated at 37 °C for 24 h. The reading of the results was carried out by measuring the diameters (mm) of the microbial growth inhibition zones generated by the gradient of the hybrid materials diffused in the culture medium. The DMSO solvent was also tested for any potential antimicrobial activity.

2.3.2. Quantitative assay of the antimicrobial activity

The quantitative assay was performed by the Mueller Hinton broth (MHB) microdilution method using 96-well plates to determine the minimum inhibitory concentration (MIC) of the tested materials, defined as the minimum amount of the chemical compound capable of inhibiting the visible growth of microbial liquid cultures. In a volume of 100 μL of MHB, serial binary dilutions of the stock solutions were achieved, ranging from 5 to 0.009 mg/mL. The wells were then seeded with 20 μL of standard microbial suspensions. Each test was run with a positive control (a row of wells containing only the culture medium inoculated with the microbial suspension) and a negative control (a row of wells containing only sterile culture medium). The plates were incubated at 37 °C for 24 h and then the results were read by the macroscopic examination. The control wells were first examined, in order to confirm the existence of a visible growth in the positive control well (the medium was cloudy as a result of microbial development) and the absence of microbial growth in the negative control (the medium remained clear, transparent). The lowest concentration which inhibited the visible growth of microbial culture (the aspect of the well-being similar with that of the negative control) was recorded as the MIC value (mg/mL) for the respective material.

https://doi.org/10.1016/j.heliyon.2019.e01333

2.3.3. Study of the influence of tested materials on the development of microbial biofilms to the inert substratum

For this purpose, after reading the MIC values, the 96-well plates were emptied, washed twice with sterile saline in order to remove the non-adherent cells, and the microbial cells which adhered to the plastic wells were fixed with 130 μL of 80% cold methanol for 5 min and stained with 1% violet crystal alkaline solution (130 μL/well) for 15 min. The staining solution was then removed, the plates were rigorously washed under tap water and the stained microbial biofilms formed on the plastic plates were re-suspended in 33% acetic acid solution, the intensity of the colored suspension being evaluated by reading the absorbance at 492 nm [5].

3. Results and discussion

3.1. X-ray diffraction

X-ray diffraction patterns of the ZnO doped with noble metals have already been reported to show peaks consistent with the hexagonal wurtzite structure of ZnO as well as additional peaks corresponding to the expected positions of the noble metal dopants [27]. X-ray diffraction patterns of the pure and noble metals doped TiO_2 are presented in Fig. 1. For the undoped TiO_2 all the diffraction peaks matched the tetragonal structure of TiO_2 (PDF 01-084-1286, anatase). In the case of the doped samples, extra peaks indicated by asterisks (*) occurred at the expected angles of Au, very similar to the case of doped ZnO. The crystallite size for the TiO_2 host material was obtained by using the Scherrer equation [29, 30] which gave a value of about 28 nm. For TiO_2 the width of the diffraction peaks become narrower when doped with Au. It is evident that the diffraction peaks labelled (105) and (211) are better separated in the Au doped TiO_2 sample than in the pure TiO_2, which implies a larger crystallite size and enhancement of crystallinity of the doped TiO_2.

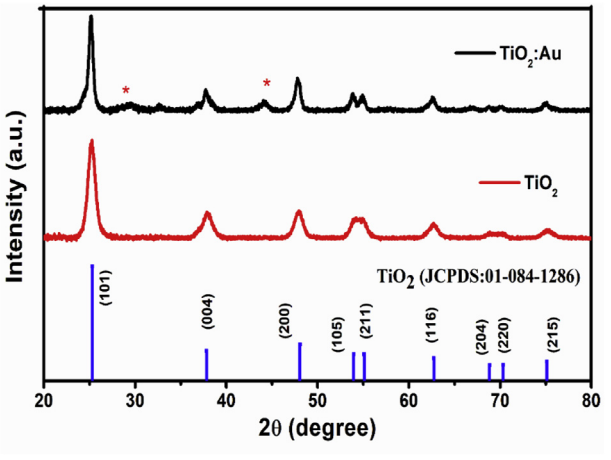

Fig. 1. XRD patterns of pure and Au doped TiO_2. Peaks marked with an asterisk correspond to Au NPs.

https://doi.org/10.1016/j.heliyon.2019.e01333

3.2. Surface morphology

The surface morphology of undoped ZnO nanomaterials produced by combustion synthesis has been reported to exhibit a flower-like structure [26]. Fig. 2 shows a SEM image of Pd doped ZnO, consisting of a mixture of nanoparticles with larger particles of several hundred nanometres. The grain size was generally higher than that observed for pure ZnO [26] and the larger grain size may be explained by NPs agglomeration. The morphology of Pd doped ZnO was found to be similar to that for ZnO doped with some other noble metals, namely Ag and Au, as shown in our previous work [28].

Fig. 3 shows the morphology of undoped and Au doped TiO_2 powders. White spots represent the accumulation of gold NPs. The effect of different dopants (B, N, Ag) was studied by Bezerra et al. [31] and they found that the morphology and grain size changed with different type and concentration of dopants.

3.3. Optical study

The absorbance of ZnO, both undoped and noble metal doped, has been reported previously [27] and absorption peaks associated with localized surface plasmon resonance (LSPR) of the noble metal NPs were observed at the corresponding wavelengths of the NPs [32, 33] while undoped ZnO showed no absorbance at wavelengths greater than 400 nm. Fig. 4(a) illustrates the absorbance of TiO_2 and Au/TiO_2. For the Au/TiO_2 sample there was some absorbance observed as a broad peak between 550-650 nm, which is attributed to the agglomeration of gold particles and corresponding localized surface plasmon resonance (LSPR) absorption.

Fig. 4(b) plots photoluminescence spectra of TiO_2 material, in the case of undoped and Au doped material. We previously reported [27] that for ZnO the PL intensity of the excitonic as well as defect emissions increased after doping with noble metals.

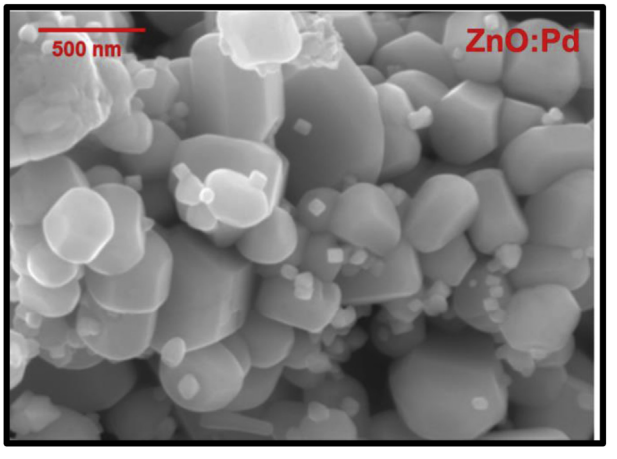

Fig. 2. SEM image of Pd/ZnO.

https://doi.org/10.1016/j.heliyon.2019.e01333

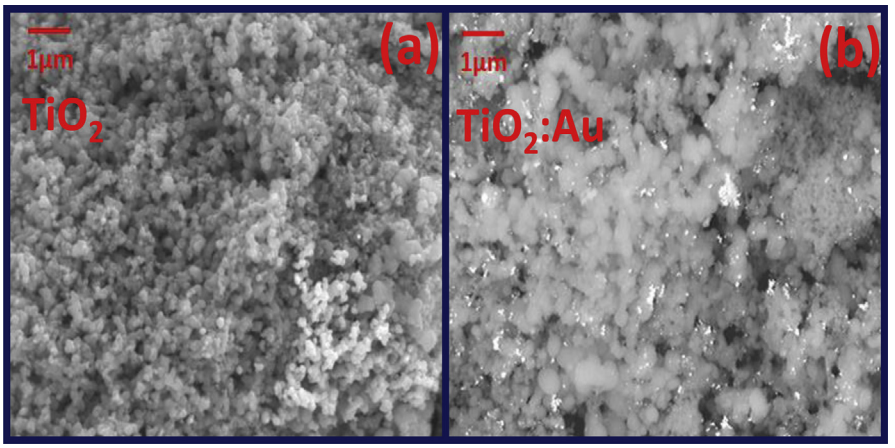

Fig. 3. SEM results of (a) undoped TiO_2 (b) TiO2 doped with Au.

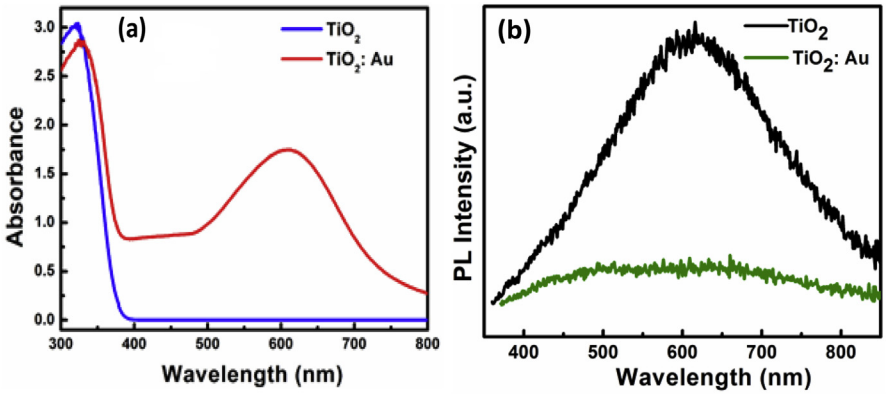

Fig. 4. (a) Absorbance and (b) PL of TiO_2 and Au/TiO_2.

This was attributed to the aggregation of noble metallic NPs in the ZnO, which act as the recombination centres, and consequently, an increase in the charge recombination [34]. The formation of Au and Pd NPs enhanced the excitonic emission while Au NPs were most effective in increasing the visible emission. In the case of pure TiO_2 (Fig. 4(b)) the defect peak is observed in the visible region centred at 600 nm. Unlike in the case of ZnO, doping the TiO_2 with Au reduces this visible defect emission. This may be due to the presence of the NPs quenching the radiative recombination process, unlike what was observed for ZnO, or it may be more plausible that the defects (concentration or form) were significantly affected by the doping of the noble material (Au) which led to decreased luminescence. Similar results for in Au/TiO_2 were reported by Bouhadoun et al. [35]. They synthesised NPs in one step using the laser pyrolysis method and described that the PL emission is consistent with the reduced radiative recombination of the photo-induced electrons trapped in the TiO_2 particle surface.

https://doi.org/10.1016/j.heliyon.2019.e01333

3.4. Antimicrobial activity

The effect of noble metal doping on antimicrobial properties of ZnO and TiO_2 materials was investigated. The study of the potential antimicrobial activity of the obtained hybrid materials was carried out toward Gram-positive and Gram-negative bacterial, as well as fungal reference strains, both in planktonic and biofilm growth state.

The qualitative assay of the antimicrobial activity of the stock solutions (10 mg/mL in DMSO) of the obtained materials revealed that ZnO group materials proved to better diffuse in the solid medium and to affect the growth of the Gram-positive *S. aureus* and *E. faecalis* strains, inducing the occurrence of significant growth inhibition zones (Table 1 and Fig. 5). Fig. 5 shows the inhibitory effect of the test chemical compounds for the Gram-positive *S. aureus* as an example. The TiO_2 and Au/TiO_2 compounds did not exhibit a visible inhibitory effect on the tested strains in this experimental model. However, this could be due to the low solubility and diffusion of these compounds in the solid culture medium.

Table 1. Microbial growth inhibition zones diameters (mm) obtained in the presence of the DMSO stock solutions of the tested materials.

Material	*S. aureus*	*E. faecalis*	*E. coli*	*P. aeruginosa*	*C. albicans*
DMSO	-	-	-	-	-
TiO2	-	-	-	-	-
Au/TiO2	-	-	-	-	-
ZnO	9	10	-	-	-
Ag/ZnO	10	10	-	-	-
Au/ZnO	10	10	-	-	-
Pd/ZnO	9	10	-	-	-

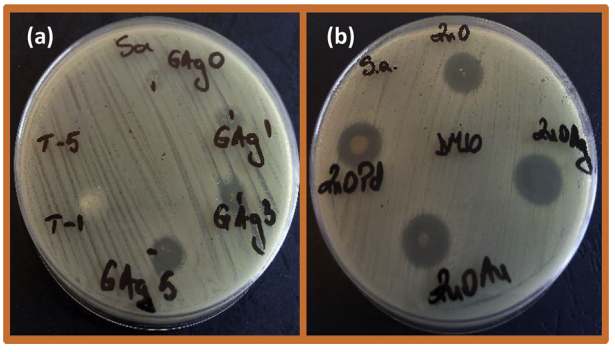

Fig. 5. Evidence of the inhibitory effect of the test substances by the qualitative method on an agar medium, the Gram-positive *S. aureus*. The test chemical compounds were (a) T-1 (TiO_2), T-5 (TiO_2:Au), GlassAgO, GlassAg1, GlassAg3, GlassAg5 and (b) ZnO:Ag, ZnO:Pd, ZnO:Au, ZnO, dissolved in DMSO, as indicated in the photographs.

https://doi.org/10.1016/j.heliyon.2019.e01333

Table 2. MICs (mg/mL) of the obtained materials toward the tested strains.

	TiO_2	Au/TiO_2	ZnO	Ag/ZnO	Au/ZnO	Pd/ZnO
S. aureus	10	5	0.078	0.039	0.078	0.039
E. faecalis	10	10	0.039	0.039	0.078	0.078
E. coli	5	2.5	0.039	0.039	0.078	0.039
P. aeruginosa	5	5	0.039	0.039	0.078	0.039
C. albicans	1.25	2.5	0.312	0.156	0.312	0.312

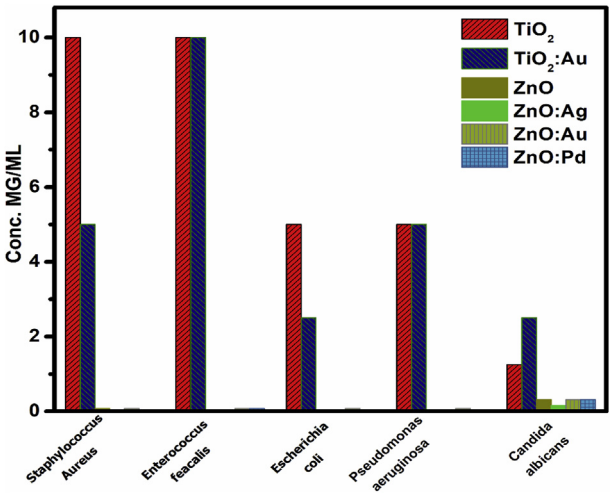

Fig. 6. MIC values obtained for test compounds against microbial reference strains.

The quantitative assay of the antimicrobial activity was performed in liquid medium. This assay assures a better and homogenous contact between the tested nanoparticles and the microbial cells and allows one to establish the MIC of the tested materials (Table 2 and Fig. 6).

The results of the quantitative assay have confirmed the qualitative screening finding, demonstrating that ZnO derived materials proved to exhibit a significantly higher antimicrobial activity, as revealed by the much lower MIC values, ranging between 0.078 and 0.039 mg/mL for all tested bacterial strains and from 0.312 to 0.156 mg/mL for the yeast strain. In case of TiO_2 materials, the Au doping slightly increased their efficiency against *S. aureus* and *E. coli* strains, as revealed by the halving of the MIC value, while for ZnO ones, doping with Ag improved the activity of ZnO NPs against *S. aureus* and *C. albicans* strains and Pd increased the efficiency of the hybrid materials against *S. aureus.* Previous studies have shown that Ag/ZnO NPs display a higher antibacterial efficacy than pure ZnO NPs towards both Gram-positive (*S. aureus*, *B. subtilis*) and Gram-negative (*E. coli* and *P. aeruginosa*) bacterial strains in planktonic growth state [5]. These results have been also confirmed in our study for *S. aureus* in planktonic growth state. It has been also observed that the

https://doi.org/10.1016/j.heliyon.2019.e01333

Ag doping of ZnO increases the efficacy of Ag/ZnO against *S. auerus* strains in a concentration dependent manner. Our previous results showed that the antibacterial activity of TiO_2 nanoparticles increased with the increasing AgNPs content, the effect being more intensive for Gram-positive bacteria [6].

Despite previous studies showing that Au/ZnO exhibited improved photocatalytic activity and antibacterial effects against *S. aureus* and *E. coli* under visible light irradiation [5, 6], we did not observe any difference between the pure ZnO and Au/ZnO nanomaterials concerning their antimicrobial features against planktonic cells. Very few studies regarding the influence of Pd on the antimicrobial features of ZnO NPs have been reported. Gondal et al. reported that loading ZnO NPs with 5% nano-Pd increased the antifungal activity of nano-ZnO against *Aspergillus* sp. and *Candida* sp. strains [5]. Our study reveals that Pd increased the inhibitory activity of ZnO against the planktonic growth of *S. aureus.*

Although the efficiency of TiO_2 materials was lower than that of ZnO materials against planktonic cells, however, they proved a similar or even improved activity against biofilm growth, the MBEC values being up to 4 times lower than the corresponding MIC values (Table 3 and Fig. 7).

Table 3. MBECs (mg/mL) of the obtained materials toward the tested strains.

	TiO_2	Au/TiO_2	ZnO	Ag/ZnO	Au/ZnO	Pd/ZnO
S. aureus	2.5	2.5	0.625	0.625	0.625	0.625
E. faecalis	5	2.5	1.25	1.25	1.25	1.25
E. coli	2.5	2.5	0.625	0.312	0.156	0.078
P. aeruginosa	1.25	1.25	1.25	1.25	1.25	1.25
C. albicans	1.25	1.25	0.312	0.156	0.312	0.312

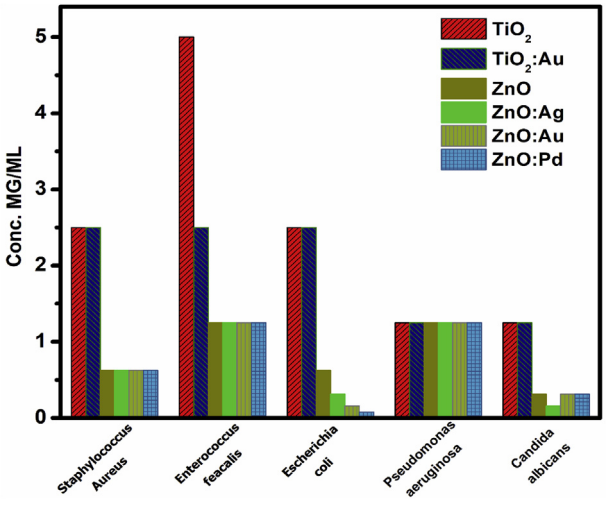

Fig. 7. The CMEB values obtained for the compounds tested against microbial germinating strains.

https://doi.org/10.1016/j.heliyon.2019.e01333

This is a very significant result, taking into account that the microbial cells grown in biofilms are much more tolerant to antimicrobial substances, the concentrations required to eradicate biofilms being up to hundreds times higher than the concentrations active on the microbial cells grown in suspension. Moreover, Au doping increased the anti-biofilm activity of TiO_2 material in the case of *E. faecalis* biofilms.

However, ZnO materials exhibited a much lower anti-biofilm activity in case of all tested bacterial strains, the MBEC values being up to 16 fold higher than the corresponding MICs. Only the antifungal activity of these materials was similar against yeast cells in planktonic and biofilm growth state. All doping of noble metals improved the anti-biofilm activity of ZnO materials against *E. coli* biofilms, decreasing the MBEC values by 8 fold in case of Pd, 4 fold in Au and 2 fold in case of Ag. The results of our study indicate only a moderate antimicrobial activity of Au doped TiO_2 NPs, as revealed by the high MIC values.

4. Conclusion

ZnO and TiO_2 nanomaterials were produced successfully by combustion synthesis. The XRD patterns revealed that tetragonal TiO_2 of anatase phase was formed. The SEM data showed that there was not uniform mixing of the noble metal dopants in the Pd/ZnO and Au/TiO_2 samples and they were agglomerated. LSPR absorption of the Au was also observed for TiO_2 samples in the range 550−650 nm. The results of the antimicrobial assays were very promising, showing a large spectrum of antimicrobial activity for all ZnO materials towards the planktonic growth of all tested Gram-positive and Gram-negative bacterial strains, with very low MIC values and the good anti-biofilm features of all doped materials, particularly of ZnO doped with Au and Pd against *E. coli* and of ZnO doped with Ag against *C. albicans* biofilm. From these results the potential that these materials have for antimicrobial applications in biomedicine and environmental protection was demonstrated.

Declarations

Author contribution statement

Trilok K. Pathak: Conceived and designed the experiments; Performed the experiments; Analyzed and interpreted the data; Wrote the paper.

R. E. Kroon: Conceived and designed the experiments; Wrote the paper.

Valentin Craciun, Marcela Popa, M. C. Chifiriuc: Performed the experiments; Analyzed and interpreted the data; Wrote the paper.

H. C. Swart: Conceived and designed the experiments; Contributed reagents, materials, analysis tools or data; Wrote the paper.

https://doi.org/10.1016/j.heliyon.2019.e01333

Funding statement

This work was supported by the South African Research Chairs Initiative of the Department of Science and Technology, the National Research Foundation of South Africa (84415), Romania/South Africa research collaboration program (104027), and the University of the Free State. R. E. Croon was supported by the National Research Foundation of South Africa (Grant Number 93214). V. Craciun was supported by the Competitiveness Operational Program 2014−2020, ANCSI/MFE, project number MIFID ID P_39_366 Cod My SMIS 104809 and INFLPR Program NUCLEU.

Competing interest statement

The authors declare no conflict of interest.

Additional information

No additional information is available for this paper.

References

[1] A.J. Huh, Y.J. Kwon, "Nanoantibiotics": a new paradigm for treating infectious diseases using nanomaterials in the antibiotics resistant era, J. Control. Release 156 (2011) 128−145.

[2] C.N.R. Rao, S.R.C. Vivekchand, K. Biswasa, A. Govindaraja, Synthesis of inorganic nanomaterials, Dalton Trans. 34 (2007) 3728−3749.

[3] R.K. Jha, P.K. Jha, K. Chaudhury, S.V.S. Rana, S.K. Guha, An emerging interface between life science and nanotechnology: present status and prospects of reproductive healthcare aided by nano-biotechnology, Nano Rev. 5 (2014) 22762., 19 pages.

[4] A. Aditya, S. Chattopadhyay, D. Jha, H.K. Gautam, S. Maiti, M. Ganguli, Zinc oxide nanoparticles dispersed in ionic liquids show high antimicrobial efficacy to skin-specific bacteria, ACS Appl. Mater. Interfaces 10 (18) (2018) 15401−15441.

[5] D. Visinescu, M. Scurtu, R. Negrea, R. Birjega, D.C. Culita, M.C. Chifiriuc, C. Draghici, J.C. Moreno, A.M. Musuc, I. Balint, O. Carp, Additive-free 1, 4-butanediol mediated synthesis: a suitable route to obtain nanostructured, mesoporous spherical zinc oxide materials with multifunctional properties, RSC Adv. 5 (121) (2015) 99976−99998.

[6] M. Radulescu, E. Andronescu, A. Cirja, A.M. Holban, L. Mogoanta, T.D. Balseanu, B. Catalin, T.P. Neagu, I. Lascar, D.A. Florea,

A.M. Grumezescu, B. Ciubuca, V. Lazar, M.C. Chifiriuc, A. Bolocan, Antimicrobial coatings based on zinc oxide and orange oil for improved bioactive wound dressings and other applications, Rom. J. Morphol. Embryol. 57 (1) (2016) 107−114. http://www.rjme.ro/RJME/resources/files/570116107114.pdf.

[7] F. Lavaee, K. Faez, K. Faez, N. Hadi, F. Modaresi, Antimicrobial and antibiofilm activity of silver, titanium dioxide and iron nano particles, Am. J. Dent. 29 (6) (2016) 315−320. PMID: 29178718.

[8] A. Nadhman, S. Nazir, M.I. Khan, S. Arooj, M. Bakhtiar, G. Shahnaz, M. Yasinzai, PEGylated silver doped zinc oxide nanoparticles as novel photosensitizers for photodynamic therapy against Leishmania, Free Radic. Biol. Med. 77 (2014) 230−238.

[9] A.M.C. Ng, et al., Antibacterial and photocatalytic activity of TiO_2 and ZnO nanomaterials in phosphate buffer and saline solution, Appl. Microbiol. Biotechnol. 97 (2013) 5565−5573.

[10] A. Kumar, A.K. Pandey, S.S. Singh, R. Shanker, A. Dhawan, Engineered ZnO and TiO_2 nanoparticles induce oxidative stress and DNA damage leading to reduced viability of Escherichia coli, Free Radical Biol. Med. 51 (2011) 1872−1881.

[11] I.S. Kim, M. Baek, S.J. Choi, Comparative cytotoxicity of Al_2O_3, CeO_2, TiO_2 and ZnO nanoparticles to human lung cells, J. Nanosci. Nanotechnol. 10 (2010) 3453−3458.

[12] R.J. Barnes, R. Molina, J. Xu, P.J. Dobson, I.P. Thompson, Comparison of TiO_2 and ZnO nanoparticles for photocatalytic degradation of methylene blue and the correlated inactivation of gram-positive and gram-negative bacteria, J. Nanoparticle Res. 15 (2013) 1−11.

[13] H. Zhang, G. Chen, Potent antibacterial activities of Ag/TiO_2 nanocomposite powders synthesized by a one-pot Sol−Gel method, Environ. Sci. Technol. 43 (8) (2009) 2905−2910.

[14] H.E. Chao, Y.U. Yun, H.U. Xingfang, A. Larbot, Study of the effect of transition metals on titanium dioxide phase transformation, J. Eur. Ceram. Soc. 23 (2003) 1457−1464.

[15] O. Akhavan, Lasting antibacterial activities of Ag−TiO_2/Ag/a-TiO_2 nanocomposite thin film photocatalysts under solar light irradiation, J. Colloid Interface Sci. 336 (2009) 117−124.

[16] U.G. Akpan, B.H. Hameed, The advancements in sol−gel method of doped-TiO_2 photocatalysts, Appl. Catal., A 375 (1) (2010) 1−11.

 https://doi.org/10.1016/j.heliyon.2019.e01333

[17] Y. Li, W. Zhang, J. Niu, Y. Chen, Mechanism of photogenerated reactive oxygen species and correlation with the antibacterial properties of engineered metal-oxide nanoparticles, ACS Nano 6 (6) (2012) 5164−5173.

[18] N. von Moos, V.I. Slaveykova, Oxidative stress induced by inorganic nanoparticles in bacteria and aquatic microalgae−state of the art and knowledge gaps, Nanotoxicology 8 (2014) 605−630.

[19] J. Kiwi, V. Nadtochenko, Evidence for the mechanism of photocatalytic degradation of the bacterial wall membrane at the TiO_2interface by ATR-FTIR and laser kinetic spectroscopy, Langmuir 21 (10) (2005) 4631−4641.

[20] Y.H. Leung, et al., Mechanisms of antibacterial activity of MgO: non-ROS mediated toxicity of MgO nanoparticles towards Escherichia coli, Small 10 (2014) 1171−1183.

[21] W. Jiang, K. Yang, R.W. Vachet, B. Xing, Interaction between oxide nanoparticles and biomolecules of the bacterial cell envelopeas examined by infrared spectroscopy, Langmuir 26 (2010) 18071−18077.

[22] J. Wang, X.M. Fan, Z.W. Zhou, K. Tian, Preparation of Ag nanoparticles coated tetrapod-like ZnO whisker photocatalysts using photoreduction, Mater. Sci. Eng. B 176 (13) (2011) 978−983.

[23] Z. Yang, P. Zhang, Y. Ding, Y. Jiang, Z. Long, W. Dai, Facile synthesis of Ag/ZnO hetrostructures assisted by UV irradiation: highly photocatalytic property and enhanced photostability, Mater. Res. Bull. 46 (2011) 1625−1631.

[24] S.M. Gupta, M. Tripathi, A review of TiO_2 nanoparticles, Chin. Sci. Bull. 56 (16) (2011) 1639−1657.

[25] A.A. Ashkarran, Antibacterial properties of silver-doped TiO_2 nanoparticles under solar simulated light, J. Theor. Appl. Phys. 4−4 (2011) 1−8. www.sid.ir/En/Journal/ViewPaper.aspx?ID=206254.

[26] Trilok K. Pathak, Ashwini Kumar, C.W. Swart, H.C. Swart, R.E. Kroon, Effect of fuel content on luminescence and antibacterial properties of zinc oxide nanocrystalline powders synthesized by the combustion method, RSC Adv. 6 (2016) 97770.

[27] Trilok K. Pathak, H.C. Swart, R.E. Kroon, Structural and plasmonic properties of noble metal doped ZnO nanomaterials, Physica B 535 (2018) 114−118.

[28] Trilok K. Pathak, R.E. Kroon, H.C. Swart, Photocatalytic and biological applications of Ag and Au doped ZnO nanomaterial synthesized by combustion, Vacuum 157 (2018) 508−513.

https://doi.org/10.1016/j.heliyon.2019.e01333

[29] R.E. Kroon, Nanoscience and the scherrer equation versus the 'Scherrer-Gottingen equation', South Afr. J. Sci. 109 (5/6) (2013). Art.#a0019 (2pp), www.scielo.org.za/scielo.php?script=sci_arttext&pid=S0038-23532013000300005#back.

[30] D.B. Hamal, K.J. Klabunde, Synthesis, characterization, and visible light activity of new nanoparticle photocatalysts based on silver, carbon, and sulfur-doped TiO_2, J. Colloid Interface Sci. 311 (2007) 514−522.

[31] P.C.S. Bezerra, R.P. Cavalcante, A. Garcia, H. Wender, M.A.U. Martines, G.A. Casagrande, J. Giménez, P. Marco, S.C. Oliveira, A. Machulek, Synthesis, characterization, and photocatalytic activity of pure and N, B or Ag doped TiO_2, J. Braz. Chem. Soc. 28 (9) (2017) 1788−1802.

[32] C. Karunakaran, V. Rajeswari, P. Gomathisankar, Combustion synthesis of ZnO and Ag-doped ZnO and their bactericidal and photocatalytic activities, Superlattice. Microst. 50 (2011) 234−241.

[33] M. Ahmad, S. Yingying, A. Nisar, H. Sun, W. Shen, M. Wei, J. Zhu, Synthesis of hierarchical flower-like ZnO nanostructures and their functionalization by Au nanoparticles for improved photocatalytic and high performance Li-ion battery anodes, J. Mater. Chem. 21 (2011) 7723−7729.

[34] Z. Zhang, H. Liu, H. Zhang, H. Dong, X. Liu, H. Jia, B. Xu, Synthesis of spindle-like Ag/ZnO heterostructure composites with enhanced photocatalytic performance, Superlattice. Microst. 65 (2014) 134−145.

[35] S. Bouhadoun, C. Guillard, F. Dapozze, S. Singh, D. Amans, J. Bouclé, N. Herlin-Boime, One step synthesis of N-doped and Au-loaded TiO2 nanoparticles by laser pyrolysis: application in Photocatalysis, Appl. Catal. B Environ. 174 (2015) 367−375.

https://doi.org/10.1016/j.heliyon.2019.e01333